

Projection through quadric mirrors made faster

Nuno Gonçalves and Ana Catarina Nogueira
Institute of Systems and Robotics - University of Coimbra
Polo 2, Pinhal de Marrocos
3030 COIMBRA

nunogon@isr.uc.pt, anacatnog@isr.uc.pt

Abstract

This paper presents a novel framework to project 3D points through curved mirrors to an image device. The problem solved is the search for the reflection point for an arbitrary vision system with a quadric shaped mirror. The main advantage claimed for the framework presented is its computer efficiency while providing better accuracy since the search for the reflection point is made in a parameterized curve that is function of a single unknown. The alternative solvers are the classical Snell Law and the Fermat Principle that, as proved in experiments, present a much slower convergence than the new method since they have a multidimensional search space rather than a unidimensional one. This new method can be used to speed up calibration of non-central catadioptric systems based on reprojection error. It can also be used for rendering purposes since it enhances the performance of the projection of points through mirrors while enhancing its accuracy, whether the mirror is part of the vision system (catadioptric camera) or if it is only a specular surface in the scene that reflects light in arbitrary directions. Another application of this framework is for illumination purposes, providing a faster way to compute reflected light direction or for the computation of the direction of the light source. Experiments in performance evaluation show the usefulness of the method presented.

1. Introduction

The projection through a specular surface is a matter of interest in several fields: computer vision, computer graphics, robotics and optics, amongst others.

Wide fields of view are extremely useful for applications such as surveillance and tracking in computer vision but also for rendering of graphics. For that purpose the directions of the light rays have to be changed in such a way as to guarantee that most of the scene can be imaged by a single sensor.

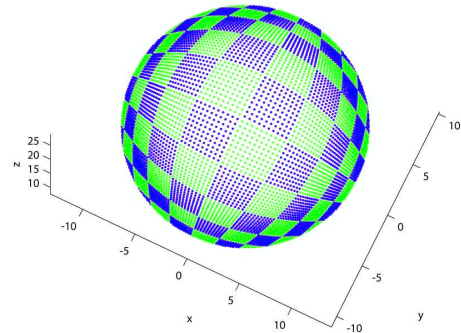


Figure 1. Reflection points of a regular grid on a spherical mirror.

Thus, changing the direction of light rays has been used in several applications and in particular for imaging systems. One of the fields that can benefit from it is panoramic imaging. Systems that use mirrors and cameras are called catadioptric. Amongst all catadioptric systems, those which use rotationally symmetric mirrors and in particular those whose mirrors are quadrics are probably the most used.

It has been shown by Nayar and Baker [1] that for quadric mirror catadioptric systems, the central projection can be obtained only for a particular position of the camera optical center, usually the focus of the quadric. However, for the general case and when this constraint is relaxed, the projection is noncentral which implies that the light rays do not intersect each other at an effective single viewpoint.

Noncentral vision systems thus have, in general, no projection model, that is, a closed form expression relating 3D world points to its corresponding pixels. However, there is extensive studies that relates a pixel with its viewing direction [11].

The existence of such a projection model is very important for rendering of scenes projected by general mirrors and also in scenes where there are specular surfaces whose reflected rays are imaged by the viewing camera - images of mirrors (despite the type of camera used). Actually the common vision systems used in rendering of images are central ones, thus reducing the freedom to project an arbi-

rary vision system or where the accuracy is relaxed to allow for fast projections through specular surfaces.

The problem we are interested in is how to find the reflection point where the light traveling from an arbitrary 3D point is reflected to another arbitrary point by a general curved mirror. This mapping between the 3D points and the image 2D points is the projection model searched for. Goncalves and Araujo have also partially addressed this problem [5].

The principles of physics are then used to understand and formulate the projection model. There are two principles that describe the reflection process. On one hand, the Snell Law states that the reflection point is the surface point whose normal vector is the bisector of the incident and reflected light rays. It also states that this normal vector to the surface is within the plane defined by the optical center, the point to be projected and the reflection point (see [7]).

On the other hand, by the laws of the Optical Geometry, it is known that the reflection point is the one that makes the light path to be the quickest one. This principle is called Fermat Principle and its first formulation is dated from 1657, based on the ancient variational principle by Hero of Alexandria (somewhere between 150 BC and 250 AD) - see [7]. Since these distances are small and no perturbation happens in the space-time, the quickest path is also the shortest one and so the total path can be minimized to achieve the reflection point.

Both Snell Law and Fermat principle are sufficient, each one *per si*, to find the reflection point. The problem is that the constraints are not explicit in the image coordinates and to solve them it is necessary to solve a multidimensional nonlinear system of equations. The dimension of the problem depends on the formulation. This problem is not difficult to solve since the expressions are well behaved for the majority of the vision systems but it is slow and computationally intense.

On the other hand, the framework we present to project 3D points to image through arbitrary quadric mirrors is fast and extremely accurate providing the parameterization of a curve where the reflection point is. Since this curve is expressed as function of only one unknown, the search problem is simpler in one or two orders of magnitude than those usually used: the classical Snell Law and Fermat Principle.

Recently Roger et al. [12] and Estalella et al. [4] have presented two different methods to compute the reflections of points through curved mirrors expressed by clouds of points or meshes. These works are not compared at this stage with our framework since they don't provide exact solutions to the projection of 3D points to image.

Our framework can additionally be extended to other types of mirrors rather than quadric surfaces since in general quadric shapes can well approximate almost all types of smooth shapes. Particularly, we intend to extend this frame-

work to non parametric mirror surfaces in future advances.

2. Problem Statement

In this section we present some notation conventions and mathematical results used throughout this paper.

Homogeneous coordinates are used and points are expressed as $\mathbf{X} = [x_1 \ x_2 \ x_3 \ x_4]^T$. The corresponding cartesian coordinate are given by $\mathbf{x} = [x \ y \ z]^T$, where $x = x_1/x_4$, $y = x_2/x_4$ and $z = x_3/x_4$. Quadric surfaces are expressed by a 4×4 symmetric matrix \mathbf{Q} . A point \mathbf{X} belongs to a quadric surface \mathbf{Q} if it respects the equation $\mathbf{X}^T \mathbf{Q} \mathbf{X} = 0$.

The next proposition concerning the coordinates of a plane is proved:

Proposition 1 *Plane coordinates defined by three non collinear points can be expressed as a linear equation in the coordinates of one of the points.*

Proof: Planes are defined by three points $\mathbf{U} = [u_1 \ u_2 \ u_3 \ u_4]^T$, $\mathbf{V} = [v_1 \ v_2 \ v_3 \ v_4]^T$ and $\mathbf{W} = [w_1 \ w_2 \ w_3 \ w_4]^T$ (generating points). We search the formulation of the plane coefficients as a linear combination of one of its generating points. Consider a plane Π and define an auxiliary matrix $\mathbf{M}_\Pi = [\mathbf{X} \ \mathbf{U} \ \mathbf{V} \ \mathbf{W}]$ composed by those three points and a generic point $\mathbf{X} = [x_1 \ x_2 \ x_3 \ x_4]^T$.

As stated by [6], since \mathbf{X} must be a linear combination of the other three points in order to belong to the plane Π , the determinant of matrix \mathbf{M}_Π must be zero. This gives us the expression of the plane in terms of the minors \mathbf{D}_{ijk} of matrix \mathbf{M}_Π . It yields $\Pi = [\mathbf{D}_{234} \ -\mathbf{D}_{134} \ \mathbf{D}_{124} \ -\mathbf{D}_{123}]^T$.

After rearranging the terms, the equation can be rewritten in the form $\Pi = \mathbf{M}\mathbf{W}$, where the matrix \mathbf{M} is symmetric. This equation is linear on \mathbf{W} . Matrix \mathbf{M} is then given by:

$$\mathbf{M} = \begin{bmatrix} 0 & u_3 v_4 - u_4 v_3 & -u_2 v_4 + u_4 v_2 & u_2 v_3 - u_3 v_2 \\ -u_3 v_4 + u_4 v_3 & 0 & u_1 v_4 - u_4 v_1 & -u_1 v_3 + u_3 v_1 \\ u_2 v_4 - u_4 v_2 & -u_1 v_4 + u_4 v_1 & 0 & u_1 v_2 - u_2 v_1 \\ -u_2 v_3 + u_3 v_2 & u_1 v_3 - u_3 v_1 & -u_1 v_2 + u_2 v_1 & 0 \end{bmatrix} \quad (1)$$

■

Consider now a pinhole camera whose optical center is the point \mathbf{C} and the intrinsic parameters matrix is the matrix \mathbf{K} . The mirror surface is given by a quadric \mathbf{Q} and is positioned freely with relation to the camera. The 3D world point \mathbf{P} is imaged by the camera and its reflection point over the mirror surface is the point \mathbf{R} . Figure 2 shows the reflection process and the notations adopted.

Without loss of generality, assume that the camera center, the quadric mirror and the 3D point to project into image are known in mirror coordinates.

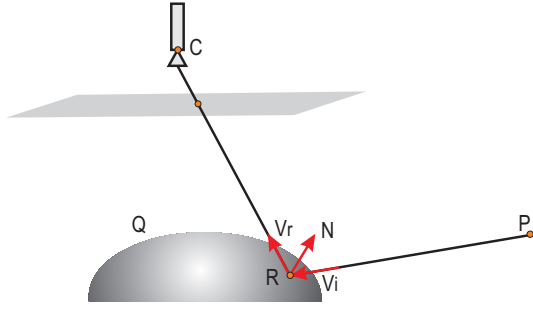


Figure 2. The light rays reflection and imaging in a vision system.

The problem we tackle in this paper is how to find the reflection point \mathbf{R} that projects the 3D point \mathbf{P} to the camera center \mathbf{C} , in a noncentral configuration. This problem can also be formulated as the search for the reflection point on a curved surface where light is reflected through a particular eye.

In the following section we review two different physical principles that can be used to compute the reflection point. In section 4 a new framework is then presented to compute the reflection point \mathbf{R} . Experiments show that this new projection model framework has better performance and computer efficiency than the other two methods: the Snell Law and the Fermat Principle.

3. Geometry of the projection

The reflection through mirrors is a well studied physical phenomenon and is explained by the Snell Law. Furthermore, the Fermat Principle states the behavior of the light rays. Both two laws can be used separately and independently from each other to compute the reflection point \mathbf{R} . We now presented the way they solve for \mathbf{R} .

3.1. Snell Law

By the Snell Law, the incident and reflected light rays are at an equal angle in relation to the normal direction to the mirror surface at the reflection point \mathbf{r} . Furthermore, the same reflection point \mathbf{r} , the camera center \mathbf{c} and the point to project \mathbf{p} define a plane that contains the normal vector. Small caps are used to denote cartesian coordinates.

Figure 3 shows the reflection process where \mathbf{v}_i is the incident light ray, \mathbf{v}_r is the reflected light ray and \mathbf{n} is the normal vector to the mirror surface. The reflection law, in cartesian coordinates, is then given by the equation:

$$\mathbf{v}_r = \mathbf{v}_i - 2(\mathbf{v}_i \cdot \mathbf{n})\mathbf{n} \quad (2)$$

To express the reflected ray \mathbf{v}_r we use an additional constraint to the equation, that all reflected light rays pass

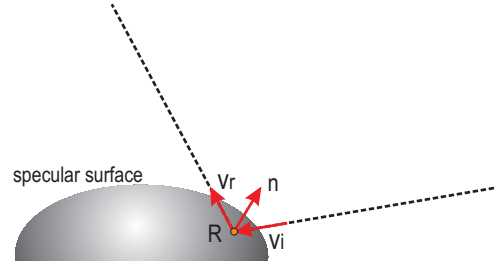


Figure 3. Specular reflection

through the optical center of the camera \mathbf{c} .

Consider $\mathbf{x} = [x \ y \ z]^T$ the generic point on the mirror surface. By substituting it in the quadratic equation, there are up to two real roots and then the appropriate one must be chosen. Since we are considering the mirror surface equation to be known, additional information about the mirror physical restriction must be available (upside or downside sheet for a two-sheets hyperbolic mirror, or the north or south hemisphere for a spherical mirror, for example). This information should be enough for the disambiguation between the two real roots. If, however, the two roots induce two valid points, the disambiguation between them is decided by the smaller value of the total distance between the 3D point and the camera optical axis, passing by the mirror surface (distance from \mathbf{p} to \mathbf{r} plus the distance from \mathbf{r} to \mathbf{c}).

Since we know the camera center \mathbf{c} and the 3D point \mathbf{p} , equation (2) can be used in the form:

$$\frac{\mathbf{c} - \mathbf{r}}{\|\mathbf{c} - \mathbf{r}\|} = \frac{\mathbf{r} - \mathbf{p}}{\|\mathbf{r} - \mathbf{p}\|} - 2 \left(\frac{\mathbf{r} - \mathbf{p}}{\|\mathbf{r} - \mathbf{p}\|} \cdot \mathbf{n} \right) \mathbf{n} \quad (3)$$

where \mathbf{n} is the normal vector to the surface at the reflection point. Its computation is straightforward.

Equation (3) is not explicit in the reflection point \mathbf{r} . It is easy to solve for \mathbf{r} but computationally hard due to all nonlinearities introduced by the norms (all incident and reflected light rays have unit norm) and by the normal vector.

The easiest way to solve it is by iterating a nonlinear multidimension minimization algorithm that iterates over the pair of coordinates (x, y) , solve for z and computes the cost function as the deviation from the Snell equation 3. The minimum should be found at the wanted reflection point \mathbf{R} .

3.2. Fermat Principle

The reflection point can also be calculated using the Fermat principle. This principle states that the light always takes the quickest path. So the reflection point is the one that minimizes the distance between the 3D point \mathbf{p} and the

camera center \mathbf{c} . Notice that for the order of magnitude of these systems, no perturbation in the space-time exists and so the quickest path is also the shortest one.

Since we also know the quadric mirror parameters, it is possible to express one of the coordinates as function of the other two. We opt to express z in relation to x and y . This is done to incorporate the mirror restriction in the equation of Fermat principle. As used in the case of the Snell Law, the coordinates of the reflection point are then expressed in cartesian coordinates by $\mathbf{r} = [r_x \ r_y \ r_z]$, where the third coordinate is given by the following equation:

$$r_z = -\frac{1}{q_{33}}(q_{13}r_x + q_{23}r_y + q_{34}) \pm \frac{1}{2q_{33}}\sqrt{D} \quad (4)$$

where the discriminant is given by:

$$D = (2q_{13}r_x + 2q_{23}r_y + 2q_{34})^2 - 4q_{33}(q_{11}r_x^2 + q_{22}r_y^2 + 2q_{12}r_xr_y + 2q_{14}r_x + 2q_{24}r_y + q_{44}) \quad (5)$$

and the appropriate root must be chosen in the same way as stated for the Snell Law.

The distances between \mathbf{r} and \mathbf{c} and between \mathbf{r} and \mathbf{p} can now be calculated and their sum minimized. The total distance is then given by:

$$d_{lightpath} = \sqrt{(r_x - c_x)^2 + (r_y - c_y)^2 + (r_z - c_z)^2} + \sqrt{(r_x - p_x)^2 + (r_y - p_y)^2 + (r_z - p_z)^2} \quad (6)$$

and r_z is given by expression (5).

Expression (6) can be analytically minimized by any known method. The expressions obtained are nonlinear and implicit in the coordinates of the reflection point. It still needs, however, a nonlinear multidimensional minimization method to compute numerically the solution.

In the following section we present a new framework for the computation of the reflection point that reduces the dimensionality of the problem and enhances the computation efficiency of the search for \mathbf{R} .

4. New projection model - QI method

From equation (3) and (6) we see that both the Snell Law and the Fermat Principle solve the problem of the reflection point. The solution is however, implicit, nonlinear, multidimensional, often unstable and computationally demanding.

In this section we present a projection model that can be applied to noncentral catadioptric vision systems composed by a quadric mirror and a perspective camera. The camera intrinsic parameters, the quadric and the pose of the camera

in relation to the mirror are assumed to be known. Homogeneous coordinates are used rather than Cartesian.

The first step to solve the problem is to characterize the reflection point.

4.1. Restrictions imposed on the reflection point

\mathbf{R} is the reflection point on the mirror surface that projects the 3D point \mathbf{P} into the image plane passing through the camera center \mathbf{C} . For such point the following three restrictions must be imposed:

1. $\mathbf{R}^T \mathbf{Q} \mathbf{R} = 0 \longrightarrow$ the point is on the quadric of the mirror surface.
2. $\mathbf{R}^T \mathbf{S} \mathbf{R} = 0 \longrightarrow$ the point is on the quadric given by $\mathbf{S} = \mathbf{M}^T \mathbf{Q}_\infty^* \mathbf{Q} + \mathbf{Q}^T \mathbf{Q}_\infty^* \mathbf{M}$ (proposition 2).

Proposition 2 *The reflection point \mathbf{R} on a quadric mirror \mathbf{Q} , reflecting a 3D world point \mathbf{P} through the point \mathbf{C} , is on the quadric surface \mathbf{S} , given by $\mathbf{S} = \mathbf{M}^T \mathbf{Q}_\infty^* \mathbf{Q} + \mathbf{Q}^T \mathbf{Q}_\infty^* \mathbf{M}$, where \mathbf{Q}_∞^* is the absolute dual quadric, the 4×4 matrix \mathbf{M} is given by expression (1) and the plane $\Pi_{\mathbf{B}}$ is defined by the 3D world point \mathbf{P} , the camera optical center \mathbf{C} and the reflection point \mathbf{R} itself. The reflection point \mathbf{R} is such that $\Pi_{\mathbf{B}} = \mathbf{M} \mathbf{R}$.*

Proof:

Let us consider two concurrent planes: $\Pi_{\mathbf{A}}$ and $\Pi_{\mathbf{B}}$. $\Pi_{\mathbf{A}}$ is the tangent plane to the quadric \mathbf{Q} at the reflection point \mathbf{R} . Its representation is given by $\Pi_{\mathbf{A}} = \mathbf{Q} \mathbf{R}$.

The plane $\Pi_{\mathbf{B}}$ is the plane defined by three points: the camera optical center \mathbf{C} , the 3D point \mathbf{P} and the reflection point \mathbf{R} on the mirror surface. As showed in section 2 the plane coordinates vector can be defined by a linear equation in the reflected point \mathbf{R} expressed by $\Pi_{\mathbf{B}} = \mathbf{M}(\mathbf{P}, \mathbf{C}) \cdot \mathbf{R} = \mathbf{M} \mathbf{R}$ (see equation (1)).

Given two planes with coordinates expressed by $\Pi_{\mathbf{A}}$ and $\Pi_{\mathbf{B}}$, the angle between them is given by its cosine expressed by equation (7), where \mathbf{Q}_∞^* is the absolute dual quadric.

$$\cos\theta = \frac{\Pi_{\mathbf{A}}^T \mathbf{Q}_\infty^* \Pi_{\mathbf{B}}}{\sqrt{(\Pi_{\mathbf{A}}^T \mathbf{Q}_\infty^* \Pi_{\mathbf{A}})(\Pi_{\mathbf{B}}^T \mathbf{Q}_\infty^* \Pi_{\mathbf{B}})}} \quad (7)$$

Since the normal to the quadric is perpendicular to the tangent plane and must be on the plane defined by the three points \mathbf{C} , \mathbf{P} and \mathbf{R} , then the two planes, $\Pi_{\mathbf{A}}$ and $\Pi_{\mathbf{B}}$, must be perpendicular. The angle between two planes is given by equation (7).

Since $\theta = \pi/2$ and substituting equations of the planes Π_A and Π_B into equation (7) it yields equation (8) which restricts the point \mathbf{R} to be on a quadric surface given by $\mathbf{S} = \mathbf{M}^T \mathbf{Q}_\infty^* \mathbf{Q}$.

$$\begin{aligned} \Pi_A^T \mathbf{Q}_\infty^* \Pi_B = 0 &\Leftrightarrow \mathbf{R}^T \mathbf{Q}^T \mathbf{Q}_\infty^* \mathbf{M} \mathbf{R} = 0 \Leftrightarrow \\ &\Leftrightarrow \mathbf{R}^T \mathbf{M}^T \mathbf{Q}_\infty^* \mathbf{Q} \mathbf{R} = 0 \quad (8) \end{aligned}$$

Notice that matrix \mathbf{S} is not symmetric as the generic quadric matrix. However, without loss of generality, matrix \mathbf{S} can be substituted by another matrix whose entries are related by $S_{ij} \leftarrow 0.5S_{ij} + 0.5S_{ji}$ or since the quadric matrix is defined up to a scale factor, we obtain a symmetric matrix by adding \mathbf{S} to its transpose. The quadric \mathbf{S} can then be computed as $\mathbf{S} = \mathbf{M}^T \mathbf{Q}_\infty^* \mathbf{Q} + \mathbf{Q}^T \mathbf{Q}_\infty^* \mathbf{M}$.

With this change the quadric remains the same and its representing matrix becomes symmetric.

■

3. The incidence and reflected angles are equal or the sum of distances to the 3D point and to the optical center of the camera is a minimum.

This third restriction imposes the choice of the reflection point on the subspace derived by the previous two constraints. For this particular choice of the reflection point one can use a reasoning based on one of the physical laws: the Snell Law or the Fermat Principle.

If the Snell Law reasoning is used, for a given point on the mirror surface, the normal vector should make an equal angle with both the incident and reflected rays. This computation is straightforward and the normal vector can be computed using the coordinates of the tangent plane to the quadric surface at the reflection point \mathbf{R} such that $\Pi_N = \mathbf{Q}\mathbf{R}$. As the normal vector is only the direction of the normal plane, its coordinates are the first three plane coordinates normalized by its norm.

The reflection point where incident and reflected rays are equal is then the solution of the following expression:

$$\text{acos}((\mathbf{c} - \mathbf{r})^T \cdot \mathbf{n}) = \text{acos}((\mathbf{p} - \mathbf{r})^T \cdot \mathbf{n}) \quad (9)$$

The alternative formulation of this third restriction is by using the Fermat Principle reasoning, that is, the total distance travelled by the light from the 3D point to the camera passing by the reflection point \mathbf{R} must be minimized. This restriction is expressed by equation 6.

Both formulations of third restriction can be used. We observed in experiments that the reasoning based on the Fermat Principle has better performance while maintaining the accuracy.

The three restrictions above can then be used to compute the reflection point on the mirror surface.

4.2. Computing the reflection point \mathbf{R}

Given the three constraints imposed to the reflection point \mathbf{R} , the problem is now how to find that point. Its explicit closed form computation is however still not possible. The first and second constraints are much similar since they restrict the point \mathbf{R} to be on quadric \mathbf{Q} (constraint (1)) and to be also on quadric \mathbf{S} (constraint (2)). This is the problem of finding the intersection of those two quadrics (a quartic in space). The third restriction constrains the point so that the incident and reflection angles are equal (Snell Law reasoning) or alternatively so that the total distance travelled by the light is minimum (Fermat Principle reasoning) and thus point \mathbf{R} must be located on the intersection curve where third restriction is met.

The general method for computing an explicit parametric representation of the intersection between two quadrics is due to Joshua Levin [9, 10]. However, the parametric representation of this method is hard to compute and is less reliable due to the high number of irrational numbers needed. Dupont et al. [3, 8] presented a modification of the Levin method to intersect quadrics with optimal number of irrationals, demonstrating that this alternative method is much more accurate than the original one.

The parametric curve given by the intersection algorithm is a function of only one parameter, say λ . Let us represent the parameterized curve by the 4×1 vector $\mathbf{X}(\lambda)$. Although nonlinear, the curve can be searched for the point where incident and reflected angles are equal, that is, where equation (9) holds or where the total distance travelled by the light is minimum. Let us call λ_0 to the value of the parameter where restriction 3 is met. The resulting reflection point is given by $\mathbf{R} = \mathbf{X}(\lambda_0)$. Notice that for non-ruled quadric mirrors equation restriction 3 has only one solution.

This method to find the reflection point \mathbf{R} on a mirror surface that projects a 3D world point \mathbf{P} to the direction of a particular point \mathbf{C} presents a major advantage over the method of using explicitly the Euclidean expressions of the mirror either using the Snell Law (equation (3)) or the Fermat Principle (equation (6)). This advantage is the fact that, once intersected the quadrics \mathbf{Q} and \mathbf{S} , the solution is given by a nonlinear equation in only one parameter. This is important for the accuracy of the solution and also to the computational efficiency of the method since the intersection of two quadrics can be computed by a non iterative method (see [3, 8] for details).

5. Discussion

The quadric surface \mathbf{S} is analytically computed and no geometrical interpretation exists for it. It is, however, important to understand the type of quadric it may be in order to enhance the performance of the intersection computation and even to characterize the intersection with the mirror: a quartic curve in space.

Since \mathbf{S} is given by $\mathbf{S} = \mathbf{M}^T \mathbf{Q}_\infty^* \mathbf{Q} + \mathbf{Q}^T \mathbf{Q}_\infty^* \mathbf{M}$, the explicit expressions of \mathbf{M} , \mathbf{Q}_∞^* and \mathbf{Q} can be replaced in the equation then yielding explicit expressions for the matrix \mathbf{S} . Notice that we consider the reference system to be placed at the origin of the mirror reference system and make no assumption on their relative orientation.

The general non-ruled quadric that express common mirrors is thus given by:

$$\mathbf{Q} = \begin{bmatrix} q_{11} & 0 & 0 & 0 \\ 0 & q_{22} & 0 & 0 \\ 0 & 0 & q_{33} & q_{34} \\ 0 & 0 & q_{34} & q_{44} \end{bmatrix} \quad (10)$$

where for different q_{11} , q_{22} , q_{33} , q_{34} and q_{44} we may have hyperbolic (of two sheets), parabolic or elliptic mirrors, including spheres.

The projection framework presented in the previous section can also be used with other types of quadric mirrors, such as cones, planes and all other, since their equations are for general quadrics. In this section we, however, discuss only the most representative mirror types - full rank quadrics.

Expanding the equation of \mathbf{S} , one can express the upper left 3×3 sub-matrix of \mathbf{S} by the following equation:

$$\mathbf{S}_u = \begin{bmatrix} 0 & m_{12}(q_{11} - q_{22}) & m_{13}(q_{11} - q_{33}) \\ m_{12}(q_{11} - q_{22}) & 0 & m_{23}(q_{22} - q_{33}) \\ m_{13}(q_{11} - q_{33}) & m_{23}(q_{22} - q_{33}) & 0 \end{bmatrix} \quad (11)$$

where m_{ij} and q_{ij} and the elements in the i -th row and j -th column of the matrices \mathbf{M} and \mathbf{Q} respectively.

As it is well known the quadric is uniquely characterized by the rank of \mathbf{S} and \mathbf{S}_u and the signal of the determinant of \mathbf{S} . Three particular cases are then analyzed in terms of \mathbf{S} , in order to characterize the quadric intersection.

Rotationally symmetric mirrors

Rotationally symmetric mirrors are the most important subclass of mirrors since they are the most common ones in practice, due to their relative ease to manufacture. For this kind of mirrors, whose symmetry is around the z-axis, one have $q_{11} = q_{22}$ and substituting it in equation (11) one obtains the following expression:

$$\mathbf{S}_u = \begin{bmatrix} 0 & 0 & m_{13}(q_{11} - q_{33}) \\ 0 & 0 & m_{23}(q_{11} - q_{33}) \\ m_{13}(q_{11} - q_{33}) & m_{23}(q_{11} - q_{33}) & 0 \end{bmatrix} \quad (12)$$

Thus, the rank of \mathbf{S} and \mathbf{S}_u are in this case 4 and 2 respectively. Computing the determinant of the quadric \mathbf{S} we achieve $\det(\mathbf{S}) = q_{11}^2 (m_{14}m_{23} - m_{13}m_{24})^2 (q_{33} - q_{11})^2$ which is always positive. We can see in [2] that the only quadric that matches these constraints is the hyperbolic paraboloid.

We conclude that for rotationally symmetric mirrors around the z-axis the quadric \mathbf{S} is always a hyperbolic paraboloid with inertia (2, 2).

Spherical mirrors

Spherical mirrors are special rotationally symmetric mirrors that are often used in practice, in robotics applications, computer vision, virtual reality in computer graphics and many others. Thus, they are important to study.

Observing equation (12) it can be easily seen that \mathbf{S}_u becomes a matrix of zeros for a spherical mirror where $q_{11} = q_{33}$. The quadric \mathbf{S} is, in this case, given by:

$$\mathbf{S} = \begin{bmatrix} 0 & 0 & 0 & m_{14} \\ 0 & 0 & 0 & m_{24} \\ 0 & 0 & 0 & m_{34} \\ m_{14} & m_{24} & m_{34} & 0 \end{bmatrix} \quad (13)$$

representing a plane with equation $m_{14}x + m_{24}y + m_{34}z = 0$ with inertia (1, 1). This plane pass on the origin of coordinates. Notice that in the case of spherical mirrors this result was already expected since any normal plane to the mirror is radial and since the plane that contains the points \mathbf{P} , \mathbf{C} and \mathbf{R} must also contains the normal vector to the quadric at the reflection point (Snell Law) and consequently must pass in the origin. The case of spherical mirrors can be used to help in the geometrical interpretation of quadric \mathbf{S} .

Aligned mirrors with the camera optical axis

Another special configuration that is commonly used for visual systems is the one where the camera axis is aligned with the symmetry axis of the rotationally symmetric mirror. In this case the camera center \mathbf{C} is of the form $\mathbf{C} = [0 \ 0 \ c_3 \ 1]^T$. Substituting it in the equation of the matrix \mathbf{M} and then in the equation of the quadric \mathbf{S} , it yields:

$$\mathbf{S} = \begin{bmatrix} 0 & 0 & p_2\Gamma_1 & p_2\Gamma_2 \\ 0 & 0 & -p_1\Gamma_1 & -p_1\Gamma_2 \\ p_2\Gamma_1 & -p_1\Gamma_1 & 0 & 0 \\ p_2\Gamma_2 & -p_1\Gamma_2 & 0 & 0 \end{bmatrix} \quad (14)$$

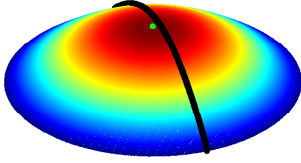


Figure 4. Intersection quartic curve of quadrics \mathbf{Q} and \mathbf{S} in black upon the quadric mirror surface.

where $\Gamma_1 = q_{33} - q_{11}$, $\Gamma_2 = c_3q_{11} + q_{34}$ and where p_i represents the i -th coordinate of the point \mathbf{P} .

Observing the expression of the quadric \mathbf{S} one can easily conclude that its rank is 2 as well as the rank of its submatrix \mathbf{S}_u . The quadric \mathbf{S} is then, for cameras aligned with the symmetry axis of a rotationally symmetric mirror, two intersecting planes that pass in the origin and has equation $(p_2x - p_1y) \cdot (\Gamma_1z + \Gamma_2) = 0$. The planes parameterized are given by $z = -\frac{\Gamma_2}{\Gamma_1}$ and $p_2x - p_1y = 0$, where the right-most plane passes at the origin and contains the z -axis. This plane also passes at the point \mathbf{P} as expected. It is then the plane defined by the symmetry axis and the point to project.

6. Experiments

In this section we perform some experiments to prove the usefulness of our framework to project light through a mirror to a vision device, mainly in terms of performance.

For visualization purposes we first project one point on a typical configuration: a rotationally symmetric hyperbolic mirror not aligned with the camera optical axis. Figure 4 shows the mirror and on its surface the quartic curve (intersection curve with the quadric \mathbf{S}) in a rotationally symmetric hyperbolic mirror not aligned with the camera axis.

One can observe from figure 4 that the intersection of the mirror with the quadric \mathbf{S} gives smooth curves on the mirror surface allowing a much more stable and quick search for the reflection point \mathbf{R} .

Concerning performance evaluation, we projected to the image a regular points grid (notice that figure 1 is an example of the reflection points of such a grid on the mirror surface) of 1600 points and measured the evaluation time for each point in three different mirrors: hyperboloid, paraboloid and sphere. All three configurations were non-central, guaranteed by off-axis positioning of the camera optical center. This test was repeated 14 times for different values of imposed pixel accuracy (reprojection error) where the accuracy in relation to ground truth was achieved by the following manner: we started from image points and back-projected them using optics. We then intersected all back-projected rays with a plane. This produced a regular grid of 3D points whose true image projections were known to be the initial image points. All points were projected to the image using our method (let us say QI method), the Snell

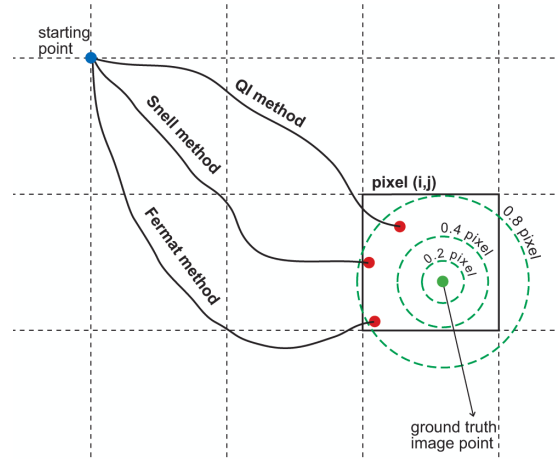


Figure 5. Process used to measure the performance of the three methods in relation to the accuracy. The dashed circles represent the vicinity of the ground truth point that the QI, Snell and Fermat methods must achieve to stop the searching algorithm.

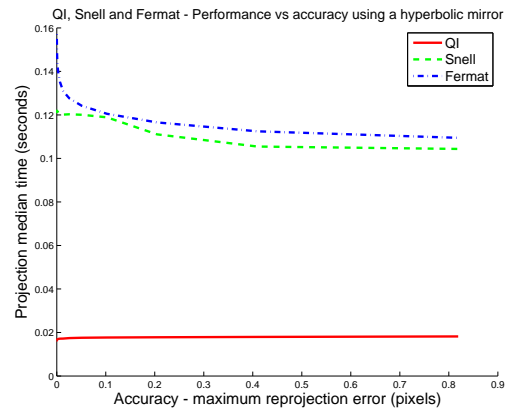


Figure 6. Performance versus accuracy in a hyperbolic mirror. The accuracy is expressed as the maximum reprojection error in pixels and the performance is the projection median time in seconds.

Law and the Fermat Principle. The nonlinear minimization algorithm was then iterated until the reprojection error was smaller than the imposed accuracy error (see figure 5 to visualize the process). The tests were performed on a Pentium Dual Core 2.4Ghz microprocessor running Matlab.

Figures 6, 7 and 8 plot the median values of the evaluation time for a point on a hyperbolic, parabolic and spherical mirror. The standard deviations of time measures were computed and they are, for all tests, of an order of magnitude lower than the median time which suggest that all points are projected in about the same elapsed time.

As can be observed from the results, the QI method that we present in this paper has always the best performance for a given accuracy, for all types of mirrors. The QI performance is in the worst case two times the Snell performance but can be up to six times the performance of Snell and Fermat methods. These results clearly prove that our method

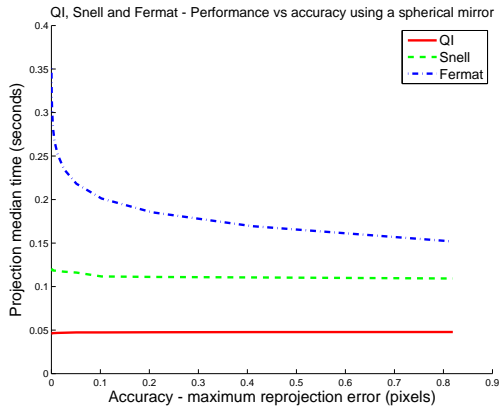


Figure 7. Performance versus accuracy in a spherical mirror. The accuracy is expressed as the maximum reprojection error in pixels and the performance is the projection median time in seconds.

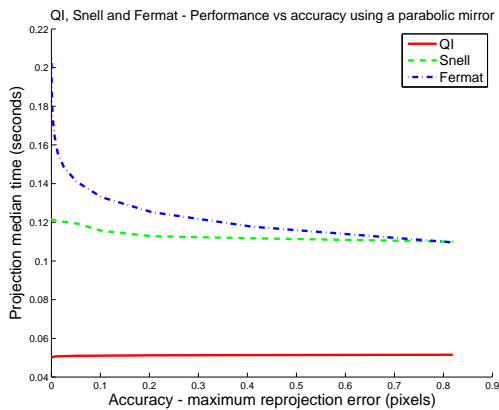


Figure 8. Performance versus accuracy in a parabolic mirror. The accuracy is expressed as the maximum reprojection error in pixels and the performance is the projection median time in seconds.

has better performance when compared with the other two.

7. Conclusion

We present in this paper a novel method to project 3D points through quadric mirrors, considering a noncentral vision system for which there are no explicit projection model. The alternative methods to solve this problem are the classical Snell Law and Fermat Principle where the reflection point is searched in a multidimensional space.

Our presented method, however, derives an unidimensional space where the reflection point can be searched for, the intersection of two quadrics. Some special configurations of this quartic curve are studied for a geometrical interpretation and also to reduce the solution complexity.

Experiments show that the performance of our method (QI) is much higher than the performance of the classical methods. This framework is thus suitable to use in computer vision for reprojection error based calibration meth-

ods or in computer graphics for rendering, illumination, visualization, augmented reality and many other applications.

In the future we want to extend the experiments to other types of mirrors, particularly to non parametric mirrors. We also want to study some other special configurations and derive simplified expressions for the intersection curve where the reflection point may be searched for (as function of the system calibration parameters). After this work to extend the framework we intend to migrate to a GPU in order to speed up the algorithm which has strong parallelization potential. Another direction to pursue is the application of this framework to computer vision and graphics problems.

Acknowledgements

The author acknowledge the support of the Portuguese Science Foundation through grant ARTHRONAV–project PTDC/EEA-ACR/68887/2006.

References

- [1] S. Baker and S. Nayar. A theory of catadioptric image formation. In *IEEE International Conference on Computer Vision*, pages 35–42, Bombay, 1998.
- [2] W. Beyer. *CRC Standard Mathematical Tables*. CRC Press, 1987.
- [3] L. Dupont, S. Lazard, S. Petitjean, and D. Lazard. *Towards the Robust Intersection of Implicit Quadrics*, chapter 5, pages 59–68. Uncertainty in Geometric Computations. Kluwer Academic Publishers, 2002.
- [4] P. Estalella, I. Martin, G. Drettakis, and D. Tost. A gpu-driven algorithm for accurate interactive specular reflections on curved objects. In *2006 Eurographics Symposium on Rendering*, 2006.
- [5] N. Gonçalves and H. Araújo. Linear solution for the pose estimation of noncentral catadioptric systems. In *7th Workshop on Omnidirectional Vision*, Rio, October 2007.
- [6] R. Hartley and A. Zisserman. *Multiple View Geometry in Computer Vision*. Cambridge University Press, 2000.
- [7] E. Hecht. *Optics*. Addison-Wesley, 1987.
- [8] S. Lazard, L. Pearanda, and S. Petitjean. Intersecting quadrics: An efficient and exact implementation. *Computational Geometry: Theory and Applications (special issue on SoCG'04)*, 35(1-2):74–99, 2006.
- [9] J. Levin. A parametric algorithm for drawing pictures of solid objects composed of quadric surfaces. *Communications of the ACM*, 19(10):555–563, 1976.
- [10] J. Levin. Mathematical models for determining the intersection of quadric surfaces. *Computer Graphics and Image Processing*, 11(1), 1979.
- [11] B. Micusik and T. Pajdla. Structure from motion with wide circular field of view cameras. *IEEE Transactions on Pattern Analysis and Machine Intelligence*, 28(7):1135–1149, July 2006.
- [12] D. Roger, N. Holzschuch, and F. Sillion. Accurate specular reflections in real-time. *Computer Graphics Forum (Eurographics'2006)*, 25(3):293–302, 2006.